Geomechanics and Engineering, *Vol. 22, No. 5 (2020) 433-439*
DOI: https://doi.org/10.12989/gae.2020.22.5.433

Reliability analysis of tunnels with consideration of the earthquakes extreme events

Mohammad Azadi*[1], S. Hooman Ghasemi[1,2] and Mohammadreza Mohammadi[1]

[1]*Department of Civil Engineering, Qazvin Branch, Islamic Azad University, Qazvin 1477893855, Iran*
[2]*Department of Civil and Environmental Engineering, Washington State University, U.S.A.*

(Received April 17, 2019, Revised February 14, 2020, Accepted July 31, 2020)

Abstract. Tunnels are one of the most important constructions in civil engineering. The damage to these structures caused enormous costs. Therefore, the safe and economic design of these structures has long been considered. However, both applied loads on the tunnels as well as the resistance of the structural members are naturally uncertain parameters, hence, the design of these structures requires considering the probabilistic approaches. This study aims to determine the load and resistant factors of lining tunnels concerning the earthquake extreme events limit state function. For this purpose, tunnels that have been designed according to the previous design codes (AASHTO Tunnel LRFD 2017) and using reliability analysis, the optimum reliability of these structures for different loading scenarios is determined. In this paper, the tunnel is considered circular. Finally, the proper load and resistance factors are calculated corresponding to the obtained target reliability. Based on the performed calibration earthquake extreme events limit state function, the result of this study can be recommended to AASHTO Tunnel LRFD 2017.

Keywords: structural reliability; tunnel; load and resistance factor design (LRFD); code calibration; seismic design

1. Introduction

Today, most probabilistic-based design codes have been developed based on the structural reliability analysis such as AASHTO Tunnel LRFD 2017, NCHRP 12-89 (2017), etc. In fact, to develop or calibrate a code, three main steps should be performed. The first step is to deliberate the uncertainties of both loads and structural resistance parameters. In doing so, several types of research have been carried out extensive studies to consider the inherent uncertainties of loads and resistance parameters. For instance, Ghasemi and Nowak (2016a) and Ghasemi *et al.* (2016) attempted to investigate the statistical parameters of weigh in motion data to propose the uncertainty behavior of vehicular loading on bridges. The second step is to determine the minimum required reliability of the structures, which is known as the target reliability. For example, Ghasemi and Nowak (2017) provided a sophisticated framework to determine the target reliability of structures. At that work, they figured out the target reliability level of steel girder bridges based on the optimization procedure with consideration of the structural importance factor. The third and final step is to calibrate the load and resistance factor corresponding to the intended target reliability level. To nail this object, Ghasemi, and Nowak (2018), provided a straightforward step-by-step method for tunnel load and resistance calibration. The main focus of this study also is to calibrate the load and resistance factors of the circular tunnel subjected to earthquakes extreme events. In addition, Hosseini *et al.* (2019) provide a method to classify the extreme events considering the vehicular collision Recently Soltani *et al.* (2020) proposed a seismic design criteria to control the structural drift using a new limit state function concerning the critical excitation.

According to the proposed study by Ellingwood (1980), the structural resistance (R) uncertainty depends on 1. Material properties, 2. Structural fabrication, and 3. The professional factor. Eq. (1) shows the uncertainties model of structural.

$$R= M\,F\,P\,Rn \tag{1}$$

where M represents the uncertainties involved the material factor that represents such as modulus of elasticity, crack stress, and chemical composition, F represents the fabrication coefficient, such as geometry. P shows the contribution of the professional factor on the resentence distribution, and Rn is the nominal resistance.

According to the existing methods, the three factors involved in the structural resistance are different for each structural component. Thus, before modeling the strength of the structure, the element selection, and the method of structural reliability analysis for any structural component, these parameters must be deliberated using statistical data collection. The statistical analyses are represented in terms of the coefficient of variation (V_R) and bias factor (λ_R) for the given structural member (Eqs. (1) and (2)).

$$V_R = \sqrt{V_{FM}^2 + V_P^2} \tag{2}$$

$$\lambda_R = (\lambda_{FM})(\lambda_P) \tag{3}$$

*Corresponding author, Ph.D.
E-mail: azadimhmm@yahoo.com

ISSN: 2005-307X (Print), 2092-6219 (Online)

where λ_{FM} is the bias factor of both fabrication and material uncertainties parameters. λ_P is the bias factor for professional variables. V_P is the coefficient of variation of professional factor, and V_{FM} is the coefficient of variation fabrication and material uncertainties. Resistance parameters are time-dependent variables, which means these statistical parameters are varied due to the deterioration of the material. Frangopol and Soliman (2015) paid attention to the fact of the material deterioration effects on the mentioned statistical parameters. This fact can be neglected at the time of structural construction. For example, Tiwari *et al.* performed the probabilistic analysis of the tunnel only with consideration of the uncertainties over the maximum value of resistance. However, Ghasemi and Nowak (2016b) noted the significant differences between the mean maximum value and the mean value of the data. Although Kroetz *et al.* (2018) attempted to provide an approximate method for reliability analysis of the tunnel, several sections of their study seem to be uneconomical due to the lack of consideration of the target reliability level.

Hamrouni *et al.* (2017) tried to presents the reliability analysis of the tunnel using the collected statistical parameters including soil behavior. They (Hamrouni *et al.* (2017)) obtained the actual non-normal distribution of the soil behavior. However, Hamrouni *et al.* (2017) followed the conventional reliability index formulation without paying attention to the new generation of the reliability index for non-normal distributions, which has been proposed by Ghasemi and Nowak (2018). In some of the reliability analyses, the soil strengths and deformations have been investigated concerning the tunnels' stability results (Cheng *et al.* 2019).

In reliability analysis, the effects of the tunnel responses should be taken into account of the extreme events. Hu *et al.* (2018) investigated the structural response of the underground structure subjected to the earthquake force associated with the water pressure effects. Banerjee and Chakraborty (2018) and Bao *et al.* (2017) considered the stability analysis of circular tunnels in saturated soil, as a function of internal friction angle and soil mass to capture the seismic behavior of tunnel. Nguyen *et al.* (2019) assessed the vulnerability of tunnels subjected to the earthquake. Patil *et al.* (2018) attempted to divulge the behavior of tunnel located within the soft soil subjected to seismic loads. Tsinidis (2017) presented a parametric study of the mode shape of the surface tunnels, which was placed in the soft soils under the effect of an earthquake loading condition. Zhang *et al.* (2017) conducted a study on the Tawarayama tunnel under the Kumamoto earthquake. The result of Zheng *et al.* (2017) classified the seismic damages into five patterns including the lining cracks, spalling and collapse of concrete lining, construction joint damage, pavement damage, and groundwater leakage. Argyroudis *et al.* (2017) found the tunnel response subjected to the vibration of the earth using a nonlinear dynamic analysis of the two dimensions. Argyroudis *et al.* (2017) concluded that the increase of the earthquake intensity caused more severe damage on the surface of the circular tunnels. Experimental studies of underground tunnels have investigated by Wang *et al.* (2018). Also, Li *et al.* (2019) conducted an experimental study to recognize the effect of the earthquakes loading on the bending behavior of the tunnel.

As a reliability point of the view, the Limit states are the boundaries between the level of safety and damage. Structures can fail in several manners. There are three levels of the structural performance known as Ultimate limit states (ULS) which is corresponding to the bending, shear and stability capacity of the structure; Serviceability limit states (SLS) refers to the deflection (Ghasemi and Nowak 2017); and Extreme Events (EE) projecting to the consideration of the extreme events such as earthquakes, flood, fire, collision, etc. One of the authors of this paper, (Ghasemi and Nowak 2018) had a significant contribution to the AASHTO tunnel LRFD 2017 code. Although AASHTO tunnel LRFD 2017 calibrated based on the consideration of ULS of the tunnel, the other limit state shall be calibrated in the future. The main innovation of this study is to calibrate the load and resistance factors of the circular tunnels with consideration of the earthquake extreme events (EE). To do so, the same circular tunnel which has been considered for the ULS calibration is taken into consideration. Accordingly, the seismic load distributions over the tunnels are determined. Eventually, the full reliability analysis is performed to first figure out what was the unknown reliability index of the current load combination of earthquake EE in AASHTO tunnel LRFD 2017. The second innovative outcome of this research is to determine the target reliability of the tunnel. And finally, the calibration process is performed to determine the load and resistance factor for earthquake extreme events (EE).

2. Modeling

In order to proceed with this research, finite element analysis is used to consider different seismic loading scenarios. The model of soil around the tunnel is considered based on the Mohr-Coulomb failure criteria. Also, the time history dynamic analyses are performed to obtain the seismic behavior of the tunnels. Finally, after performing analyses, the output results are represented in terms of the axial, shear, and bending moment for different elements of the tunnel. To perform the finite element analysis, a 2-D model of the circular tunnel has been created using the "tunnel designer" toolbar inside a plate object. The meshing procedure has been generated using a robust triangulation procedure. Herein this study, the basic soil elements have been utilized as 6-Node triangular elements, which estimate the shape function using three-points Gaussian integration.

The edge soil boundaries were assumed fully fixed conditions. However, the special boundary conditions have been applied for earthquake motion to reduce the reflection of the wave at the model boundaries. In doing so, the compliant base boundary condition has been applied to the very bottom layer. Also, a free filed boundary condition has been assumed for the entire of the lateral boundaries to make the ground feasible to shake due to the earthquake motion. The interface element also has used to model the boundary between the soil and the circular tunnel.

2.1 Input parameters in modeling

In this study, 78 models are generated with the

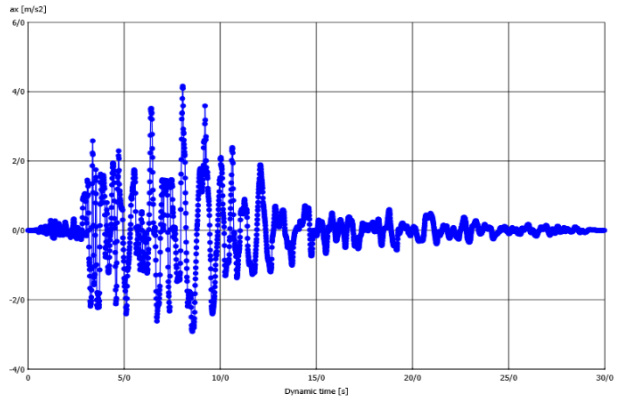

(a) Accelerogram of the Northridge earthquake

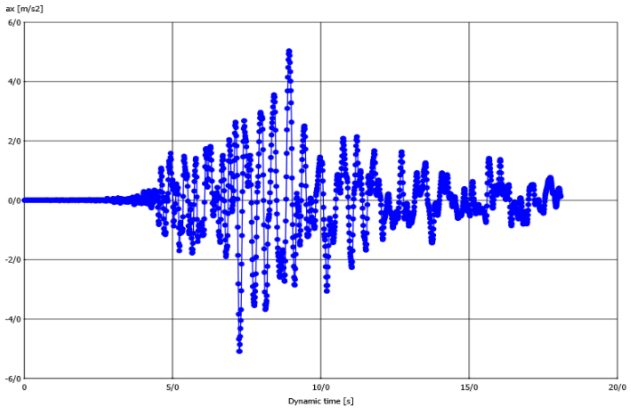

(b) Accelerogram of the Kobe earthquake

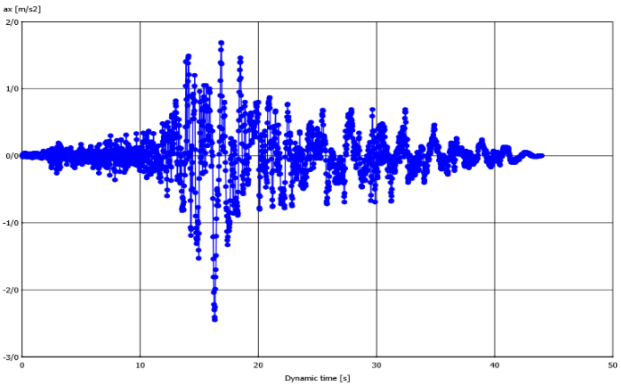

(c) Accelerogram of the Landers earthquake

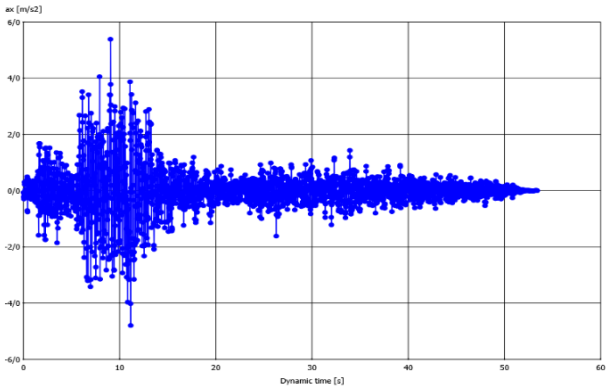

(d) Accelerogram of the Manjil earthquake

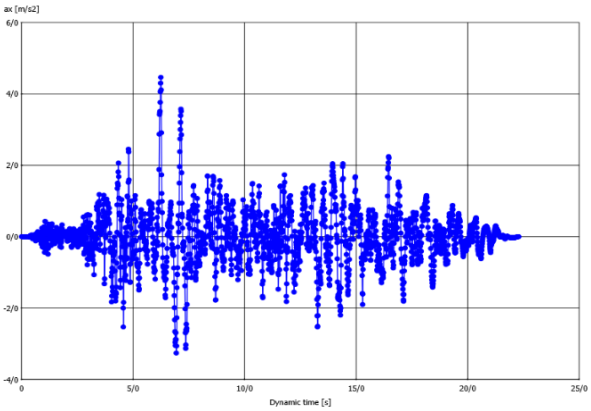

(e) Accelerogram of the Superstition Hills earthquake

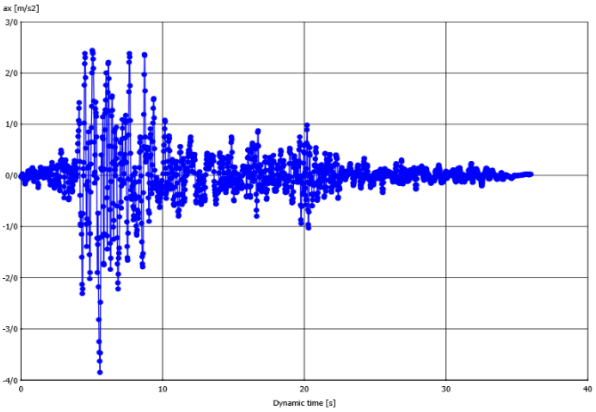

(f) Accelerogram of the Cape Mendocino earthquake

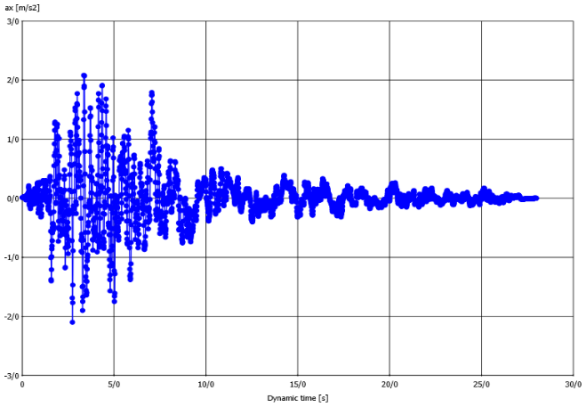

(g) Accelerogram of the San Fernando earthquake

Fig. 1 Accelerogram of considered earthquakes

Table 1 Soil properties

γ_{SAT}	Permeability	Modulus of Elasticity	Poisson Ratio	Cohesion	Friction angle	Dilatancy angle
kN/m^3	m/day	kN/m^2	---	kN/m^2	Degree	Degree
21	8.64	3.5*10^4	0.35	0	35	5

Table 2 Characteristics of the tunnel

EA	EI	Thickness of Lining	Weight of Lining (per meter)
kN/m	kN.m^2/m	m	kN/m/ m
8.216×10^6	6.16*10^4	0.3	7.5

Table 3 Calculated values for vertical and vertical load at different depths

Depth ft. (m)	The horizontal load due to the weight of the soil (top) (kPa)	The horizontal load due to the weight of the soil (middle) (kPa)	The horizontal load due to the weight of the soil (bottom) (kPa)	The vertical load due to the weight of the soil (kPa)
54 (16.46)	77.16	92.87	108.6	180.9
60.3 (8.38)	86.70	101.8	117.5	201.8
65.9 (20.09)	94.28	110.0	125.7	221.1
68.5 (20.88)	97.80	113.5	129.2	229.3
68.7 (20.94)	98.26	114.0	129.7	230.4
70 (21.34)	101.5	117.3	133	238.2

difference of several parameters including two main concerns 1- different earthquakes and 2- the variable depth of the tunnel (distance between the surface and the crown of the tunnel). In all models, the input parameters for the soil are considered the same. The specification of the materials and geometrical characteristics of the models are presented in Tables 1 and 2**.** In the modeling, six elevations have modeled (see Figure 1). In this study, H and D represent the height of the soil over the tunnel crown and diameter of the tunnel, respectively. In this study, D value assumed equal to 3.6 ft and values of H is 54 ft (16.46 m), 60.3 ft (18.38 m), 65.9 ft (20.09 m), 68.5ft (20.88 m), 68.7 ft (20.94 m), 70 ft (21.34 m) (Ghasemi and Nowak 2018).

2.1.1 Static loads

Static analysis, which consists of the six cases, is stated in each of the aforementioned height model, which is done for 36 cases as follows:

1) load due to soil weight vertically: the load caused by the weight of soil on the tunnel is perpendicular to the side of the tunnel, causing central and axial forces and bending moment in the tunnel lining. To calculate the soil weight on the tunnel for use in the software, Eq. (4) is used.

$$P_v = (\gamma_{sat} - \gamma_w)\, h \tag{4}$$

where P_v is active stress and h is depth to the crown of the tunnel. In this equation, h is the height of the soil to the crown of the tunnel. The calculated values are shown in Table 3.

2) Horizontal load due to the weight of the soil: the part of the load due to the weight of the soil on the tunnel is horizontal. This part deals with the ratio of the lateral stress factor to the tunnel lining. To model the horizontal load due to the weight of the soil using Eq. (5) for the three depths of the tunnel, the tunnel center and the tunnel floor are calculated and imported into the software. The calculated values present in Table 3.

$$P_a = K_0(\gamma_{sat} - \gamma_w)\, h \tag{5}$$

where K_0 is the coefficient of at-rest earth pressure and it is considered $K_0 = 1 - sin\ (35^\circ)$.

3) Vertical surcharge: The surcharge of the tunnel cover is considered to be an extension of the length of the tunnel. To model the vertical surcharge, a five-story building has been designed with a weight of 50 kPa.

4) Horizontal surcharge: To model the horizontal surcharge in the tunnel, a building with a weight of 50 kPa was considered to be calculated using Eq. (6).

$$Force = k_0\, q, \qquad q = 50\ kPa \tag{6}$$

5) Live load of vehicles: The overhead of the traffic within the tunnel is equivalent to 0.87 kN /m^2. This value is based on the LRFD Ordinance 2017.

6) Hydraulic pressure of water: in this section, underground water level is considered in the surface, and using Plaxis software the hydrostatic pressure is modeled.

2.1.2 Dynamic Load

To perform seismic analysis of seven earthquake records (according to Table 4), 49 dynamic analyses due to the elevation models mentioned in the previous sections are carried out in this research. Because of the possibility of the noise returned into the model and making errors, the adsorption boundaries have been used around the model. The earthquake load is considered over the bedrock. In this way, the impact of alluvium in the analysis is also considered. The accelerograms used for analyses are depicted in Figs. 1-8. The detailed specifications of the records are also presented in Table 4.

Table 4 Earthquake specifications used in the modelings

	Magnitude	Duration (sec)
Northridge-01 1994-01-17 12:31	6.69	29.98
KOBE 01/16/95 2046, NISHI-AKASHI	6.90	18.09
Landers 1992-06-28 11:58	7.28	43.98
Manjil 06/20/90, Manjil	7.40	53.40
Superstition Hills-02 1987-11-24 13:16	6.54	22.29
Cape Mendocino 1992-04-25 18:06	7.01	35.98
San Fernando 1971-02-09 14:00	6.61	27.99

3. Methodology

3.1 Load combination related to the earthquake's extreme events

Table 5 Load factors provided in Tunnel AASHTO LRFD 2017

	Load Factor	
Loads	Min	Max
Dead	1.25	0.90
Other dead	1.50	0.65
Earth Pressure	1.35	0.75
Surcharge	1.35	0.75
Live	1.75	1.75
Water Pressure	1.00	1.00
Earthquakes	1.00	1.00

Table 6 Proposed target reliability

Failure Mode	β_T
Moment	0.00
Shear	2.25
Compression	4.00

Table 7 Proposed new load factors

	Load Factor	
Loads	Min	Max
Dead	1.00	0
Other dead	1.00	0
Earth Pressure	1.00	0
-Surcharge	1.00	0
Live	1.00	0
Water Pressure	1.00	0
Earthquakes	1.00	0

Limit states are the restrictions between the level of the sound and damage. Structures can fail in several manners. There are three levels of the structural performance known as Ultimate limit states (ULS) which is corresponding to the bending, shear and stability capacity of the structure; Serviceability limit states (SLS) refers to the deflection (Ghasemi and Nowak 2017); and Extreme Events (EE) projecting to the consideration of the extreme events such as earthquakes, flood, fire, collision, etc.

The main attempt of this research is to first assess the inherent target reliability level of a circular tunnel with consideration of earthquakes extreme events (EEE). Then, based on the new proposed target reliability the new load factors for the considered load combination of EEE are represented.

The code calibration is performed based on the analyzed tunnel with the following assumption:

Radius of tunnel = 11 ft. [3.35 meter])

Cover (ranged between 54 to 71 ft. [~16.5 to 21.5 meters]).

The general design provisions are considered according to the Tunnel AASHTO LRFD 2017. Accordingly, the reliability indices are computed for reinforced concrete tunnel associated with the presented load factors in Tunnel AASHTO LRFD 2017, which are tabulated in Table 5.

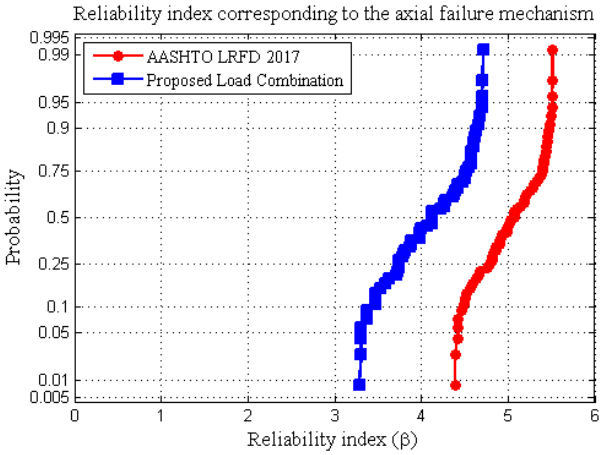

Fig. 2 Reliability index corresponding to the axial failure mechanism

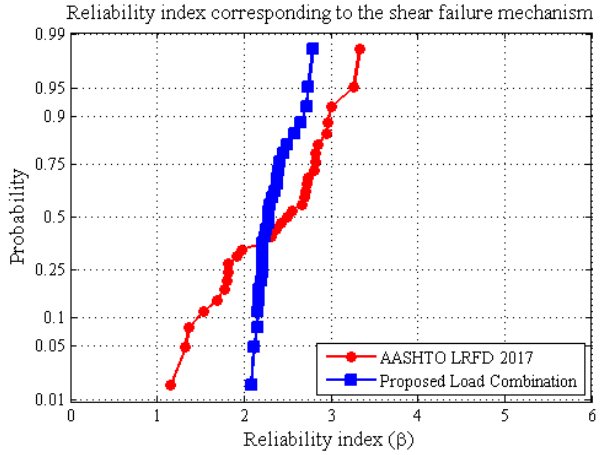

Fig. 3 Reliability index corresponding to the shear failure mechanism

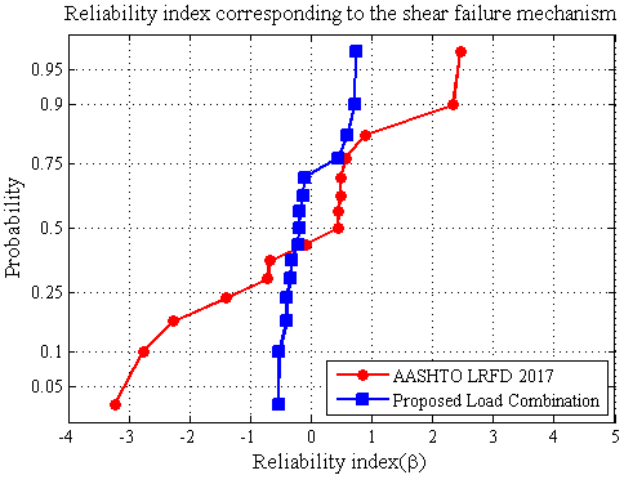

Fig. 4 Reliability index corresponding to the flexural failure mechanism

In Tunnel AASHTO LRFD 2017 the resistance factors vary from $\varphi = 0.90$ for the moment, $\varphi = 0.75$ for axial load carrying capacity.

It should be noted that all statistical parameters of the

soil and structures were given from our previous research (Ghasemi and Nowak 2018)

It should be noted that the nominal value of resistance is computed based on the factored loads.

Based on the given lifetime theory proposed by Ghasemi and Nowak (2017), a new target reliability index is chosen for 150 years for a tunnel. Meanwhile, the new target reliability is taken using a standard deviation far from the mean value of the target reliability. Therefore, the acceptable Target Reliability, β_T, is ranged between 0 to 4 for EEE. Table 6 shows the considered target reliability for the tunnel.

Eventually, using the calibration process the recommended load factors are computed, which are tabulated in Table 7.

Reliability indices variation for both presented load factors and available load factors for EEE in AASHTO Tunnel LRFD (2017) shows the distinct constant-ability of the proposed reliability indices in this research (see Fig 2-4). It worth mentioning, one of the main characteristics of choosing the target reliability and new load factors in the Code calibration process (Ghasemi and Nowak 2018).

Also, it should be stated that the considered limit state function refers to the earthquakes extreme events considering the failure modes due to the moment, shear, and axial forces. Also, seven applied earthquakes load is extracted with statistical analyses over the given seven earthquakes. Therefore, the research is expected to be extended by consideration of more seismic excitations or consideration of the critical excitation (Ghasemi and Ashtari 2014, Ghasemi *et al.* 2013 and Ashtari Ghasemi 2013). Also, the proposed target reliability needs for more sophisticated analysis which was conducted by Ghasemi (2014).

4. Conclusions

This paper was intended to calibrate the load factors of tunnel concerning the earthquakes extreme events limit state. In doing so, the statistical analysis over the given earthquakes was conducted to determine the seismic behavior of the tunnel. The main objective of this research was to determine the target reliability level of the current available LRFD Tunnel Design code (2017) with consideration of the earthquake extreme events. Accordingly, a new load combination was proposed to maintain the reliability level in a range of the target value and also corresponding to the consistency of the achieved reliability indices. As it was observed, for all considered tunnel elements, the calculated reliability indices followed a consistency spectrum level. After several calibration iterations, this paper proposed a new load combination for the earthquake extreme event limit state associated with the homogeneous spectrum of the target reliability indices.

It should be noted that, in this presented study, the reliability level of a series of the considered circular tunnels with a specific range of the mentioned dimensions was investigated. Also, the severity level of the earthquake was not categorized based on the power and intensity of those individual earthquakes. However, the mentioned limitations can be investigated in a future study.

References

AASHTO LRFD (2017), *Tunnel Design and Construction Guide Specifications*.

Ashtari, P. and Ghasemi, S.H. (2013), "Seismic design of structures using modified nonstationary critical excitation", *Earthq. Struct.*, **4**(4), 383-396. http://doi.org/10.12989/eas.2013.4.4.383.

Argyroudis, S., Tsinidis, G., Gatti, F. and Pitilakis, K. (2017), "Effects of SSI and lining corrosion on the seismic vulnerability of shallow circular tunnels", *Soil Dyn. Earthq. Eng.*, **98**, 244-256. https://doi.org/10.1016/j.soildyn.2017.04.016.

Banerjee, S.K. and Chakraborty, D. (2017), "Stability analysis of a circular tunnel underneath a fully liquefied soil layer", *Tunn. Undergr. Sp. Technol.*, **78**, 84-94. https://doi.org/10.1016/j.tust.2018.04.024.

Bao, X., Xia, Z., Ye, G., Fu, Y. and Su, D. (2017), "Numerical analysis on the seismic behavior of a large metro subway tunnel in liquefiable ground", *Tunn. Undergr. Sp. Technol.*, **66**, 91-106. https://doi.org/10.1016/j.tust.2017.04.005.

Cheng, H.Z., Chen, J., Chen, R.P. and Chen, G.L. (2019), "Reliability study on shield tunnel face using a random limit analysis method in multilayered soils", *Tunn. Undergr. Sp. Technol.*, **84**, 353-363. https://doi.org/10.1016/j.tust.2018.11.038.

Ellingwood, B. (2008), Development of a probability-based load criterion for American National Standard A58, Building code requirements for minimum design loads in buildings and other structures, US Department of Commerce, National Bureau of Standards.

Ghasemi, S.H. and Nowak, A.S. (2018), "Reliability analysis of circular tunnel with consideration of the strength limit state", *Geomech. Eng.*, **15**(3), 879-888. https://doi.org/10.12989/gae.2018.15.3.879.

Ghasemi, S.H. and Nowak, A.S. (2017), "Target reliability for bridges with consideration of ultimate limit state", *Eng. Struct.*, **152**, 226-237. https://doi.org/10.1016/j.engstruct.2017.09.012.

Ghasemi, S.H., Nowak, A.S. and Parastesh, H. (2016), "Statistical parameters of in-a-lane multiple truck presence and a new procedure to analyze the lifetime of bridges", *Struct. Eng. Int.*, **26**(2), 150-159. https://doi.org/10.2749/101686616X14555428758849.

Ghasemi, S.H. and Nowak, A.S. (2016a), "Reliability analysis for serviceability limit state of bridges concerning deflection criteria", *Struct. Eng. Int.*, **26**(2), 168-175. https://doi.org/10.2749/101686616X14555428758722.

Ghasemi, S.H. and Nowak, A.S. (2016b), "Mean maximum values of non-normal distributions for different time periods", *Int. J. Reliabil. Safety*, **10**(2), 99-109. https://doi.org/10.1504/IJRS.2016.078381.

Ghasemi, S.H. and Ashtari, P. (2014), "Combinatorial continuous non-stationary critical excitation in MDOF structures using multi-peak envelope functions", *Earthq. Struct.*, **7**(6), 895-908. http://doi.org/10.12989/eas.2014.7.6.895.

Ghasemi, S.H. and Nowak, A.S. and Ashtari, P. (2013), "Estimation of the resonance-response factor regarding to the critical excitation methods", *Proceedings of the 11th International Conference on Structural Safety & Reliability, ICOSSAR*, New York, U.S.A.

Hamrouni, A., Dias, D. and Sbartai, B. (2017), "Reliability analysis of shallow tunnels using the response surface methodology", *Undergr. Sp.*, **2**(4), 246-258. https://doi.org/10.1016/j.undsp.2017.11.003.

Hosseini, P., Ghasemi, S.H., Jalayer, M. and Nowak, A.S. (2019), "Performance-based reliability analysis of bridge pier subjected to vehicular collision: Extremity and failure", *Eng. Fail. Anal.*, **106**, 104176. https://doi.org/10.1016/j.engfailanal.2019.104176.

Hu, J., Chen, Q. and Liu, H. (2018), "Relationship between earthquake-induced uplift of rectangular underground structures and the excess pore water pressure ratio in saturated sandy soils", *Tunn. Undergr. Sp. Technol.*, **79**, 35-51. https://doi.org/10.1016/j.tust.2018.04.039.

Kroetz, H.M., Do, N.A., Dias, D. and Beck, A.T. (2018), "Reliability of tunnel lining design using the hyperstatic reaction method", *Tunn. Undergr. Sp. Technol.*, **77**, 59-67. https://doi.org/10.1016/j.tust.2018.03.028.

Li, X., Zhou, X., Hong, B. and Zhu, H. (2019), "Experimental and analytical study on longitudinal bending behavior of shield tunnel subjected to longitudinal axial forces", *Tunn. Undergr. Sp. Technol.*, **86**, 128-137. https://doi.org/10.1016/j.tust.2019.01.011.

National Corporative Highway Research Program (2002), NCHRP 12-89, Report No. 483.

Nguyen, D.D., Park, D., Shamsher, S., Nguyen, V.Q. and Lee, T.H. (2019), "Seismic vulnerability assessment of rectangular cut-and-cover subway tunnels", *Tunn. Undergr. Sp. Technol.*, **86**, 247-261. https://doi.org/10.1016/j.tust.2019.01.021.

Patil, M., Choudhury, D., Ranjith, P.G. and Zhao, J. (2018), "Behavior of shallow tunnel in soft soil under seismic conditions", *Tunn. Undergr. Sp. Technol.*, **82**, 30-38. https://doi.org/10.1016/j.tust.2018.04.040.

Soltani, M.H., Ghasemi, S.H, Soltani, A., Lee, J.Y., Nowak, A.S. and Jalilkhani, M., (2020), "State-of-the-art reliability analysis of structural drift control corresponding to the critical excitations", *J. Earthq. Eng.*, In Press.

Tiwari, G., Pandit, B., Latha, G.M. and Babu, G.S. (2017), "Probabilistic analysis of tunnels considering uncertainty in peak and post-peak strength parameters", *Tunn. Undergr. Sp. Technol.*, **70**, 375-387. https://doi.org/10.1016/j.tust.2017.09.013.

Tsinidis, G. (2017), "Characteristics of rectangular tunnels in soft soil subjected to transversal ground shaking", *Tunn. Undergr. Sp. Technol.*, **62**, 1-22. https://doi.org/10.1016/j.tust.2016.11.003.

Wang, G., Yuan, M., Miao, Y., Wu, J. and Wang, Y. (2018), "Experimental study on seismic response of underground tunnel-soil-surface structure interaction system", *Tunn. Undergr. Sp. Technol.*, **76**, 145-159. https://doi.org/10.1016/j.tust.2018.03.015.

Zhang, X., Jiang, Y. and Sugimoto, S. (2018), "Seismic damage assessment of mountain tunnel: A case study on the Tawarayama tunnel due to the 2016 Kumamoto Earthquake", *Tunn. Undergr. Sp. Technol.*, **71**,138-148. https://doi.org/10.1016/j.tust.2017.07.019.

JS

List of notations

D	diameter of
F	fabrication factor
H	height of the soil over the tunnel crown
h	depth to the crown
K_0	the coefficient of at-rest earth pressure
P	professional factor
P_a	horizontal load due to the weight of
P_v	active stress
R	resistance parameter
V_{FM}	coefficient of variation fabrication and material uncertainties
V_P	coefficient of variation of professional factor
V_R	coefficient of variation of resistance
β	reliability index
β_T	target reliability
γ_{sat}	Saturated soil density
γ_w	Water density
λ_R	bias factor of resistance
λ_{FM}	bias factor of both fabrication and material uncertainties parameters
λ_p	bias factor for professional variables